Paper AAS 03-516

Effect of Thrust Profile on Velocity Pointing Errors of Spinning Spacecraft

Daniel Javorsek II

US Air Force
Luke AFB, Arizona

James M. Longuski

School of Aeronautics and Astronautics
Purdue University
West Lafayette, Indiana

AAS/AIAA Astrodynamics Specialists Conference

Big Sky, Montana **August 3-7, 2003**

AAS Publications Office, P.O. Box 28130, San Diego, CA 92198

AAS 03-516

EFFECT OF THRUST PROFILE ON VELOCITY POINTING ERRORS OF SPINNING SPACECRAFT

Daniel Javorsek II* and James M. Longuski†

Abstract

During axial thrusting maneuvers, spacecraft and rockets are often spin-stabilized to ameliorate the effect of undesired transverse torques from thruster offset and misalignment. The velocity-pointing errors due to these undesired torques are inversely proportional to the square of the spin rate. Recent work shows that the spin-stabilized axial thrust maneuver can be improved considerably by softening the ignition transient (for example, by increasing the thrust gradually from zero to maximum, rather than having a nearly instantaneous jump to maximum thrust). In previous work it is found that a linear-ramp thruster profile (for ignition and for burnout) provides a significant reduction in velocity-pointing errors. One advantage of this type of thrust profile is that it permits much smaller spin rates, which reduces the propellant mass required for spin up and spin down. We show that deviations from the linear thrust profile, such as a sinusoidal or an exponential profile, do not have significant effects on the inherent advantage of softening the ignition transient. However, increasing the duration of the thrust transient (in the profiles we examine) provides the greatest reduction in velocity-pointing errors.

INTRODUCTION

Spacecraft are frequently spin-stabilized during large axially-thrusting maneuvers[1]. High spin rates are often required since off-axis forces induce body-fixed torques transverse to the spin axis. These off-axis forces come from a variety of sources including engine center-of-mass (CM) offset and/or misalignment (see Fig. 1). Such body-fixed torques cause velocity pointing errors since the angular momentum and velocity vectors are perturbed in inertial space. In many cases the thrust profile (and hence the

*Capt., U.S. Air Force, 56th Fighter Wing, Luke AFB, Arizona 85309.

†Professor, Associate Fellow AIAA, Member AAS. School of Aeronautics and Astronautics, Purdue University, West Lafayette, IN 47907-1282.

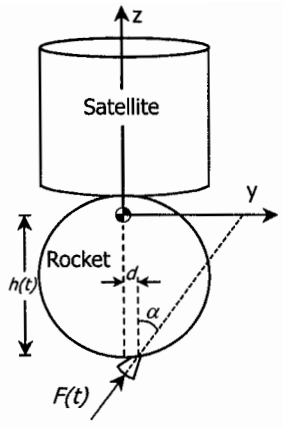

Figure 1 Generic spacecraft configuration highlighting engine misalignment and offset.

torque profile) can be modeled as a step function, leading to the velocity-pointing error, ρ, depicted in Fig. 2a. Recently, a new method has been proposed[2,3] to significantly reduce the pointing error by employing the thrust profile shown in Fig. 3. The resulting behavior of the angular momentum vector, H, is that it spirals about the desired pointing direction, Z, which consequently leads to the ΔV lying along Z, as shown in Fig. 2b.

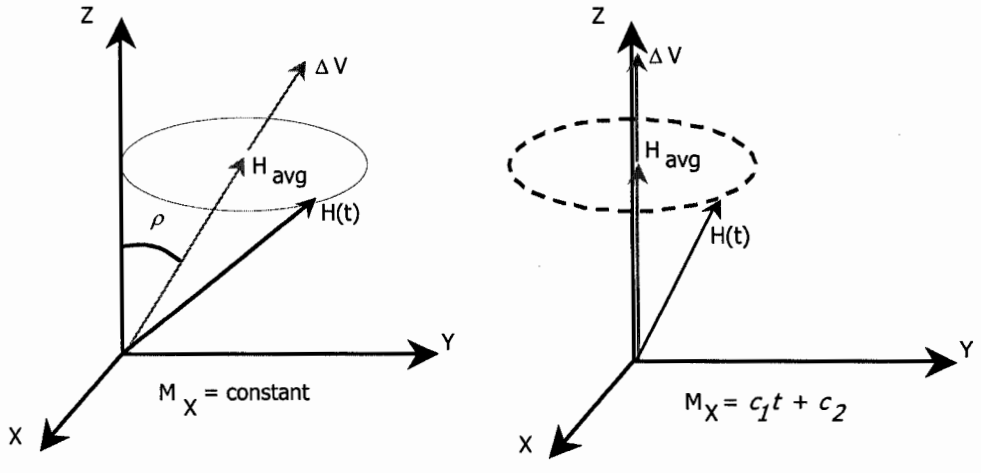

(a) (b)

Figure 2 Motion of the angular momentum vector in inertial space for the (a) constant and (b) linearly increasing thrust profiles.

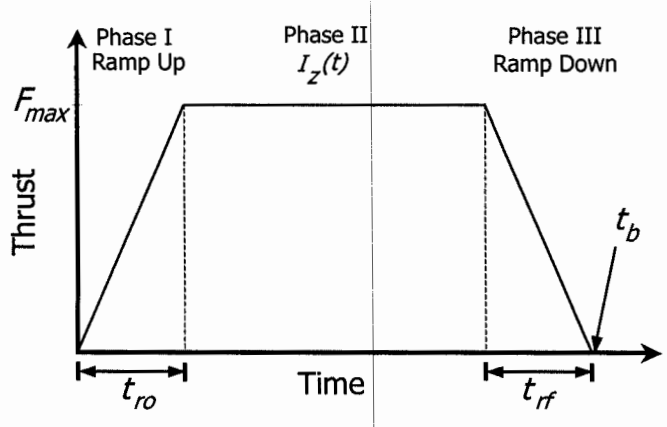

Figure 3 The trapezoidal thrust profile discussed in previous work. Phase I is the ignition transient phase which is the focus of the present paper.

A simple method can be used to quickly deduce the main results of Refs. [2] and [3]. We start with Euler's law,

$$\mathbf{M} = \frac{d\mathbf{H}}{dt}. \tag{1}$$

where M and $\mathbf{H}$ denote the spacecraft moment and angular momentum respectively. Assuming we have a single transverse body-fixed torque M_x which remains in the inertial XY plane we may rewrite Eq. (1) as

$$\begin{aligned} \dot{H}_X &= M_X = M_x \cos \Omega t \\ \dot{H}_Y &= M_Y = M_x \sin \Omega t \\ \dot{H}_Z &= M_Z = 0 \end{aligned} \tag{2}$$

where Ω is the spacecraft spinrate (and is assumed to be held constant), and the subscripts X, Y, Z and x, y, z denote the orthogonal inertial and body-fixed coordinates respectively.

For the case where the thrust profile is a step function M_x is a constant and solving Eq. (2) gives

$$
\begin{aligned}
H_X &= \frac{M_x \sin \Omega t}{\Omega} \\
H_Y &= \frac{M_x}{\Omega}(1 - \cos \Omega t) \\
H_Z &= I_z \Omega
\end{aligned}
\tag{3}
$$

where I_z is the principle moment of inertia (PMOI) along the z axis.

Table 1 provides the numerical values for an example and represent common spacecraft parameters[4,5]. The motion of the resulting angular momentum vector in inertial space is then given in Fig. 4. From the figure we notice that the center of the circle is shifted by an angle $\rho = 82.5$ mrad. Since the direction of the ΔV follows the average angular momentum vector[1], there is a velocity pointing error of 82.5 mrad introduced into the system due to the body-fixed torque caused by small engine misalignment and offset.

In Fig. 3 we see that the thrust profile is broken into three phases. Different simplifying assumptions can be made for each phase and the subsequent analytical solution can be derived[2,3]. Phase I is the ignition transient and includes the rise to maximum thrust. Since this first phase is short with respect to the total burn time we assume that the principle moment of inertia $I_z = I_{z0}$, mass $m = m_0$, and distance to the center of mass $h = h_0$ are equal to their initial values for the analytical solution. During the second phase the thrust is held constant, $h = (h_0 - h_f)/2$, $m = (m_0 - m_f)/2$, and I_z is linearly decreasing. Here the subscript f denotes the final values. In the final phase of the trapezoidal thrust scheme the engine is gradually shut down so that the angular momentum vector is returned to its original direction.

The reduction in velocity-pointing error[2,3] is significantly influenced by the ignition transient burn time t_r. If we constrain t_r such that

Table 1
SPACECRAFT NUMERICAL SIMULATION DATA

Variable	Notation	Quantity
Maximum Thrust Force	F_{max}	76,100 N
Maximum CM offset	d	0.02 m
Thrust Misalignment	α	0.25 deg
Distance from throat of engine nozzle to CM	h_0	0.80 m
Initial spinrate	Ω	70 rpm
Initial PMOI about z axis	I_{z0}	401 kg-m^2
Mass	m	2,500 kg

$$t_r > \frac{2\pi}{\Omega} \tag{4}$$

the velocity-pointing error can be reduced by nearly two orders of magnitude.

Since the ignition transient phase of the trapezoidal thrust scheme provides the greatest reduction in velocity-pointing errors, we concentrate on this phase in the present paper. In the succeeding sections we first evaluate the effect of increased t_r on the velocity-pointing errors and then investigate the effects of different ignition transient thrust profiles.

DURATION EFFECTS

Analytical Solution

The solutions for the trapezoidal thrust scheme are broken up by phase and given in terms of the components of the angular momentum vector $\mathbf{H} = (H_X, H_Y, H_Z)$. For VPES the ignition transient is described in terms of a linearly increasing thrust and the solution to Euler's Law gives

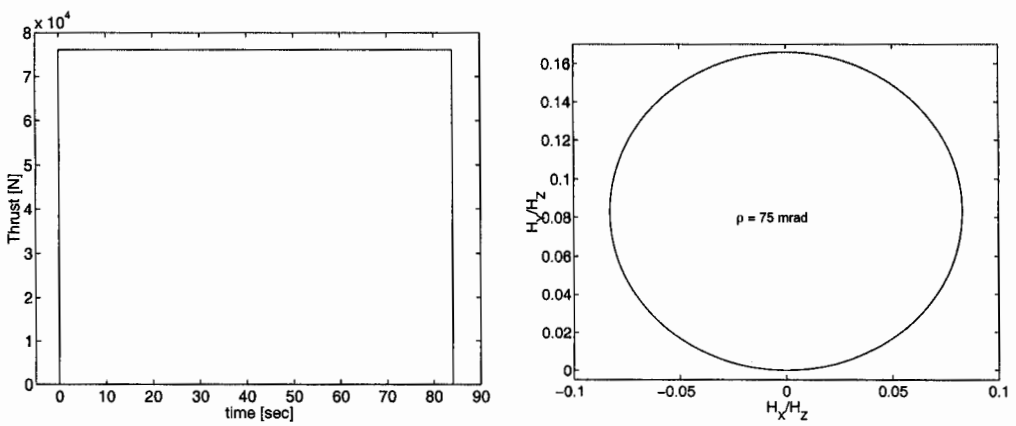

(a) (b)

Figure 4 Thrust profile for a step function emulated by current engines. (b) Analytical solution for the motion of the angular momentum vector in inertial space.

$$H_X = (h_0 \sin\alpha + d\cos\alpha)\left(\frac{F_{max}}{t_{r0}\Omega_0}\right)\left[\frac{\cos(\Omega_0 t)}{\Omega_0} + t\sin(\Omega_0 t) - \frac{1}{\Omega_0}\right]$$

$$H_Y = (h_0 \sin\alpha + d\cos\alpha)\left(\frac{F_{max}}{t_{r0}\Omega_0}\right)\left[\frac{\sin(\Omega_0 t)}{\Omega_0} - t\cos(\Omega_0 t)\right] \tag{5}$$

$$H_Z = I_{z0}\Omega_0$$

From the equations we note that as t_{r0} increases the time it takes for the thrust to reach the maximum value F_{max} increases. This linearly increasing thrust is governed by the simple equation

$$F(t) = \left(\frac{F_{max} - F_{min}}{t_{r0}}\right)t + F_{min}. \tag{6}$$

The angle we desire is the velocity-pointing error γ. Recall that the velocity change in inertial space during thrusting maneuvers is realized through integration of the acceleration equations

$$\begin{bmatrix} a_X \\ a_Y \\ a_Z \end{bmatrix} = A \begin{bmatrix} F_x/m \\ F_y/m \\ F_z/m \end{bmatrix} \tag{7}$$

Here F_x, F_y, F_z represent body-fixed forces and A is the transformation matrix which switches from orthogonal inertially-fixed coordinates (denoted by X, Y, Z subscripts) to body-fixed coordinates (denoted by x, y, z subscripts). There are 12 forms of Euler angle rotation matrices which provide the attitude of a spacecraft. Using a type 1: 3-1-2 rotation, A is given by

$$A = \begin{bmatrix} c\phi_x c\phi_z - s\phi_x s\phi_y s\phi_z & -s\phi_x c\phi_y & c\phi_x s\phi_z + s\phi_x s\phi_y c\phi_z \\ s\phi_x c\phi_z + c\phi_x s\phi_y s\phi_z & c\phi_x c\phi_y & s\phi_x s\phi_z - c\phi_x s\phi_y c\phi_z \\ -c\phi_y s\phi_z & -s\phi_y & c\phi_y c\phi_z \end{bmatrix}. \tag{8}$$

Here ϕ are the Euler angles, and c and s denote the cosine and sine respectively.

If the desired ΔV is along the inertial Z axis, integration of Eq. (7) provides the components of the velocity change in inertial space $(\Delta V_X, \Delta V_Y, \Delta V_Z)$. We then normalize the transverse velocities ΔV_X and ΔV_Y to define the velocity-pointing error angles γ_X and γ_Y by

$$\begin{aligned} \tan\gamma_X &= \Delta V_X/\Delta V_Z \\ \tan\gamma_Y &= \Delta V_Y/\Delta V_Z \end{aligned} \tag{9}$$

where ΔV_X and ΔV_Y are much smaller than ΔV_Z. For analytic solutions this error can be approximated by the average angular momentum vector since the velocity imparted to the spacecraft aligns with the average $\mathbf{H}$ [1-3]. As a result, we introduce ρ which is the angle between the angular momentum vector and the inertial Z axis,

$$\begin{aligned} \tan \rho_X &= H_X/H_Z \\ \tan \rho_Y &= H_Y/H_Z \end{aligned} \tag{10}$$

where H_X, H_Y, H_Z are given in Eq. (5) for the ignition transient phase of the burn. During the second phase of the burn, in which the thrust is held constant, $\mathbf{H}$ is given by

$$\begin{aligned} H_X &= \frac{(h_0 \sin\alpha + d\cos\alpha)\, F_{max} \sin(\Omega t)}{\Omega} \\ H_Y &= \frac{(h_0 \sin\alpha + d\cos\alpha)\, F_{max} \left[1 - \cos(\Omega t)\right]}{\Omega} \\ H_Z &= I_{z0}\Omega. \end{aligned} \tag{11}$$

Numerical Solution

A definition of all the constants used in the analysis is provided in Table 1. The motion of the angular momentum vector in inertial space is given in Fig. 5. The constant thrust solution is provided in Fig. 5b for comparison. Examination of this

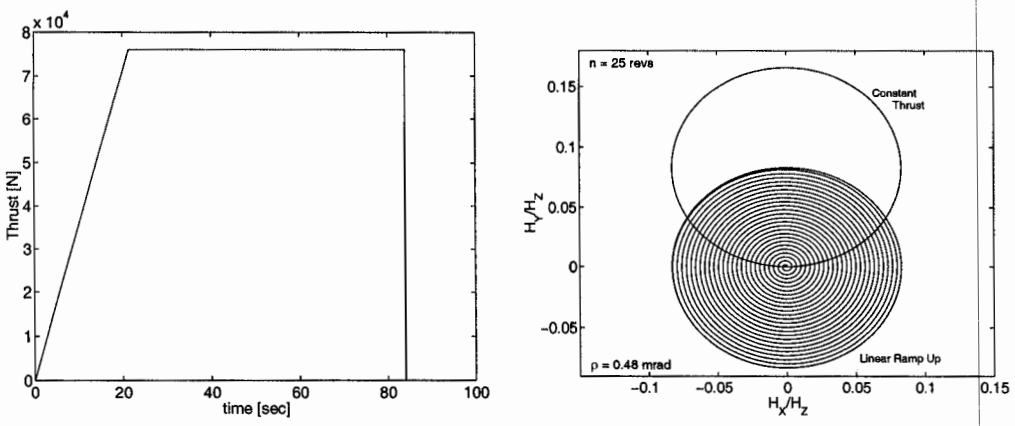

(a) (b)

Figure 5 (a) Thrust profile for a linearly increasing ignition transient phase followed by a constant thrust phase. (b) Projection of the angular momentum vector in inertial space for this thrust profile.

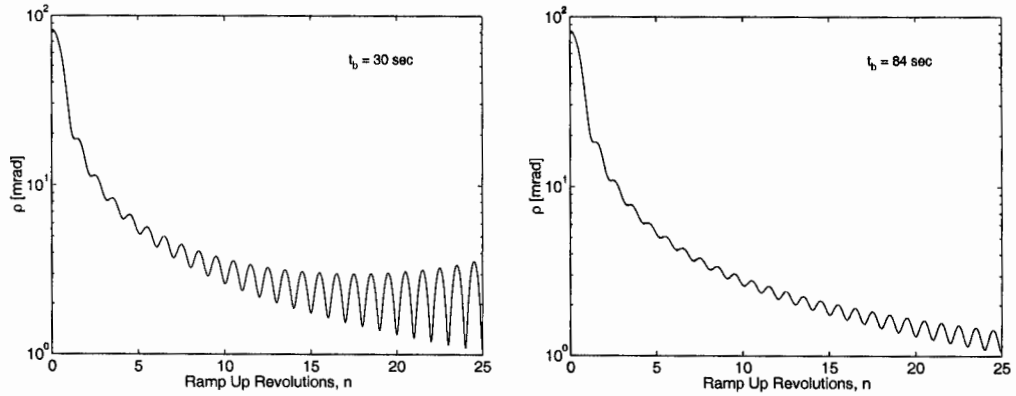

Figure 6 Velocity-pointing Error ρ as a function of the number of revolutions for the ignition transient phase of the trapezoidal thrust scheme with (a) $t_b = 30$ sec and (b) $t_b = 84$ sec.

figure shows that for the case where 25 intermediate revolutions were used during the ignition transient phase, the average angular momentum is centered closer to the origin thereby reducing the pointing error. Where the step function of the previous section gave a $\rho = 82.5$ mrad for a $t_b = 85$ sec, the ramp up profile provides over two orders of magnitude reduction in the error with $\rho = 0.48$ mrad.

Applying this concept for different values of t_r such that more revolutions are realized during the ramp up implies greater precision may be obtained. Figure 6 displays this behavior as well as giving two examples for different total burn times.

Notice that as t_r increases the velocity-pointing error decreases for different total burn times t_b. This of course makes sense since increasing t_r allows the body-fixed moments to be averaged out throughout the engine runup. We also note that increasing the total burn time allows more averaging during Phase II of the trapezoidal thrust scheme, thereby dampening the fluctuations in n.

PROFILE EFFECTS

Different methods may be used to soften the ignition transient phase of the thrust profile. In an attempt to find a thrust profile that optimizes the velocity-pointing we consider several different ignition transient thrust histories. In each case analyzed below the motion of the average angular momentum vector in the new analytic solutions is along the Z axis, thereby implying the velocity-pointing error will be small and may be approximated by the average $\mathbf{H}$ [1-3].

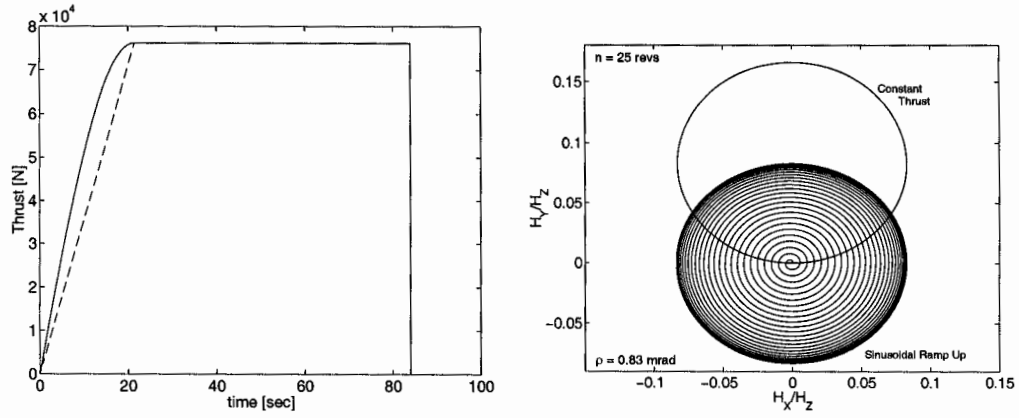

(a) (b)

Figure 7 (a) Thrust profile for a sinusoidal ignition transient followed by a constant thrust phase. (b) Corresponding analytical solution for the motion of the angular momentum vector in inertial space.

Sinusoidal Ignition Transient

For the sinusoidal ignition transient the body-fixed torque is given by

$$M_x = (h_0 \sin\alpha + d\cos\alpha) F_{max} \sin\left(\frac{\pi}{2t_r} t\right). \tag{12}$$

Solving Eq. (2) we arrive at the angular momentum vector components

$$\begin{aligned} H_X &= \frac{(h_0 \sin\alpha + d\cos\alpha) F_{max}}{2(\pi^2/4t_r^2 - \Omega^2)} \left(\frac{\pi}{t_r} - \eta\cos\kappa t - \kappa\cos\eta t\right) \\ H_Y &= \frac{(h_0 \sin\alpha + d\cos\alpha) F_{max}}{2(\pi^2/4t_r^2 - \Omega^2)} (\eta\sin\kappa t - \kappa\sin\eta t) \\ H_Z &= I_{z0}\Omega \end{aligned} \tag{13}$$

where $\eta = (\pi/2t_r) + \Omega$ and $\kappa = (\pi/2t_r) - \Omega$. Figure 7a shows the thrust profile with the dashed line for the linear case provided as a reference. As with the linear case before Fig. 7b gives the motion of the angular momentum vector in inertial space projected onto the X-Y plane. As with Fig. 5, the constant thrust case is provided for reference. In this case we notice that $\rho = 0.83$ mrad which is slightly greater than that of the linear ignition transient.

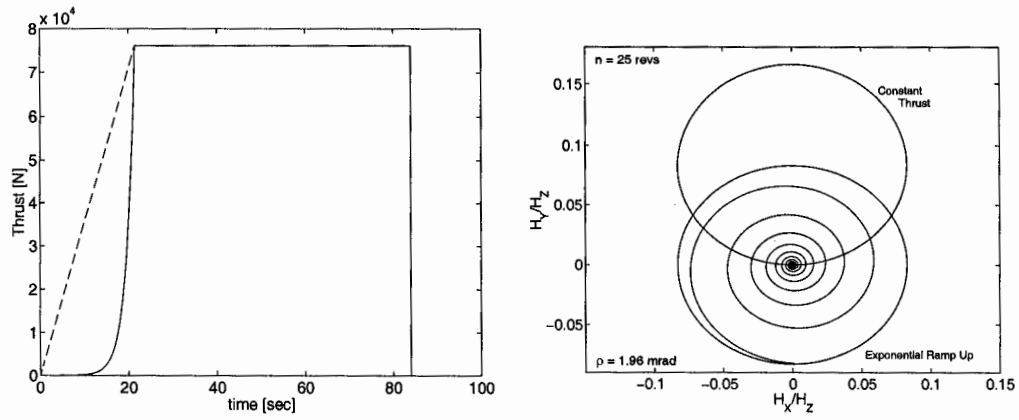

(a) (b)

Figure 8 Thrust profile for an exponential ignition transient followed by a constant thrust phase. (b) Corresponding analytical solution for the motion of the angular momentum vector in inertial space.

Exponential Ignition Transient

For the exponential ignition transient the body-fixed torque is given by

$$M_x = (h_0 \sin\alpha + d\cos\alpha)(e^{kt} - 1) \tag{14}$$

where $k = \ln(F_{max})/t_r$. Solving Eq. (2) we arrive at the angular momentum vector components

$$\begin{aligned} H_X &= (h_0 \sin\alpha + d\cos\alpha)\left[\frac{e^{kt}(k\cos\Omega t + \Omega\sin\Omega t) - k}{k^2+\Omega^2} - \sin\Omega t\right] \\ H_Y &= (h_0 \sin\alpha + d\cos\alpha)\left[\frac{e^{kt}(k\sin\Omega t - \Omega\cos\Omega t) + \Omega}{k^2+\Omega^2} + \cos\Omega t - 1\right] \\ H_Z &= I_{z0}\Omega. \end{aligned} \tag{15}$$

As with the previously discussed ignition transients, Figure 8 provides both the thrust profile and the corresponding projection of the angular momentum vector in inertial space. In this case the velocity pointing error is $\rho = 1.96$ mrad which is even greater than the sinusoidal case. From the figures we notice that the exponential ignition transient deviates from the ideal linear profile by a larger amount and thereby gives a larger velocity-pointing error.

Table 2 is included to provide a direct comparison of the different profiles as well as to show the dramatic impact increased duration has on reduction of pointing errors. In this table, all calculations were numerically performed with $I_z(t)$, $h(t)$, and $m(t)$ allowed to vary throughout the burn. We also have included jet damping so that the results presented are most closely aligned with expected results. For the case of the constant thrust one may notice that allowing the variables mentioned above to vary as well as including jet damping lowers the error from 82.5 to 75 mrad.

CONCLUSIONS

We conclude the following:

1.) Increasing the duration of the ignition transient phase allows the off axis torques to be more completely averaged and results in a greater reduction of velocity-pointing errors (see Table 2). Precise control of the duration also can provide added reduction although to a much smaller degree.

2.) Of the profiles inspected, the linear ignition transient provides for the greatest reduction in pointing errors with a minimal value of 0.48 mrad. However it should be emphasized that all profiles inspected were of the same magnitude (see Table 2).

From this study we show that the bulk of error reduction arises by increasing the ignition transient duration with secondary effects from precise control of the thrust profile. This is a positive outcome for applications to current technologies since in general it is easier to control the duration than precisely design a profile. In any real system, deviations from the ideal linear profile will undoubtedly be present and since velocity pointing errors are rather insensitive to variations in the profile itself such deviations should not greatly impact the vehicle velocity vector.

Table 2
EFFECTS OF DURATION AND PROFILE ON POINTING ERROR

Profile	n	ρ [mrad]
Constant Thrust	0	75
Ramp	1	4.0
Ramp	2	1.9
Ramp	25	0.48
Sinusoidal	25	0.83
Exponential	25	1.96

ACKNOWLEDGEMENTS

The views expressed in this paper are those of the authors and do not reflect the official policy or position of the U.S. Air Force, U.S. Department of Defense, or the U.S. Government.

REFERENCES

1. J. M. Longuski, T. Kia, and W. G. Breckenridge, "Annihilation of Angular Momentum Bias During Thrusting and Spinning-Up Maneuvers," *Journal of the Astronautical Sciences*, Vol. 37, No. 4, 1989 pp. 433–450.
2. D. Javorsek II and J. M. Longuski, "Velocity Pointing Errors Associated with Spinning Thrusting Spacecraft," *Advances in the Astronautical Sciences: Proceedings from the 1999 AAS/AIAA Astrodynamics Specialist Conference* Vol. 103, 2000 pp. 2347–2364.
3. D. Javorsek II and J. M. Longuski, "Velocity Pointing Errors Associated with Spinning Thrusting Spacecraft", *Journal of Spacecraft and Rockets*, Vol. 37, No. 3,2000 pp. 359–366.
4. R. N. Knauber, "Thrust Misalignment of Fixed-Nozzle Solid Rocket Motors," *Journal of Spacecraft and Rockets*, Vol. 33, No. 6, 1996 pp. 794–799.
5. J. H. Saleh, D. E. Hastings, and D. J. Newman, "Spacecraft Design Lifetime," *Journal of Spacecraft and Rockets*, Vol. 39, No. 2, 2002 pp. 244–257.